

7-1-2011

FOURIER FINITE ELEMENT ANALYSIS OF LATERALLY LOADED PILES IN ELASTIC MEDIA Internal Geotechnical Report 2011-1


William Higgins

University of Connecticut - Storrs, william.higgins@uconn.edu

Dipanjan Basu

University of Connecticut - Storrs, dipanjan.basu@uconn.edu

Follow this and additional works at: http://digitalcommons.uconn.edu/cee_techreports

 Part of the [Civil Engineering Commons](#), [Environmental Engineering Commons](#), and the [Geotechnical Engineering Commons](#)

Recommended Citation

Higgins, William and Basu, Dipanjan, "FOURIER FINITE ELEMENT ANALYSIS OF LATERALLY LOADED PILES IN ELASTIC MEDIA Internal Geotechnical Report 2011-1" (2011). *Technical Reports*. 2.
http://digitalcommons.uconn.edu/cee_techreports/2

**FOURIER FINITE ELEMENT ANALYSIS OF LATERALLY
LOADED PILES IN ELASTIC MEDIA**

Internal Geotechnical Report 2011-1

William Higgins and Dipanjan Basu

Department of Civil and Environmental Engineering
University of Connecticut

Storrs, Connecticut

July 2011

Copyright by

William Higgins and Dipanjan Basu

2011

SYNOPSIS

Laterally loaded piles are analyzed using the Fourier finite element method. Pile response was observed to be a function of the relative stiffness of pile and soil and of the pile slenderness ratio. The analysis is mostly performed for piles embedded in elastic soil with constant and linearly varying modulus although the pile response in two-layer soil profiles is also investigated. Equations describing pile head deflection, rotation and maximum bending moment are proposed for flexible long piles and stubby rigid piles. The design equations were developed after plotting the pile responses as functions of pile-soil stiffness ratio and pile slenderness ratio. These plots can also be used as design charts. Design examples illustrating the use of the analysis are also provided.

KEYWORDS: pile foundation, lateral load, finite element analysis, elastic solution, design

INTRODUCTION

Structures resting on piles are frequently subjected to horizontal forces due to wind, traffic and seismic activities. The horizontal forces acting on tall or heavy structures like high rise buildings, bridge abutments and earth-retaining structures are often of very large magnitude. Offshore structures like quays and harbors are also subjected to large lateral forces arising out of wind, waves and ship berthing. The horizontal forces eventually get transmitted to the piles, which are analyzed considering a concentrated force and/or moment acting at the pile head. Even in structures where piles are used to resist vertical forces only, there may exist moments due to load eccentricities caused by faulty construction. Consequently, proper analysis and design of piles subjected to lateral forces and moments is very important in order to ensure the stability and serviceability of various structures.

Numerous research studies, both theoretical and experimental, have been performed on laterally loaded piles for more than six decades. The early theoretical works stem from the concept of representing soil by discrete springs with the soil subgrade modulus as the spring constant. However, the conventional subgrade modulus approach was modified to account for plastic deformation of soil by incorporating nonlinearity in the soil springs (Matlock and Reese 1960, McClelland and Focht 1958). Further development of this method led to the well known p-y method in which nonlinear p-y curves (p is the pressure at the pile-soil interface due to lateral pile deflection y) are prepared for different pile depths from available soil data and given as inputs to the discretized pile nodes for obtaining numerical solutions of the pile-displacement differential equation following an iterative algorithm (Reese and Cox 1968, Matlock

1970, Reese et al. 1974, 1975). However, the p-y curves are not mechanistically related to the strength and stiffness of soil. These curves are developed by giving them as inputs to the numerical simulations of some field pile-load tests and adjusting the curves until the results of the numerical simulations match the field results. Thus, the p-y curves represent the soil resistance against lateral pile movement on an ad hoc basis. Consequently, these curves are actually site specific and there are evidences in the literature where the p-y method produced inaccurate results (Kim et al. 2004).

The continuum approach, in which the pile is assumed to be embedded in a continuum, is conceptually superior to the spring approach of the p-y method. Poulos (1971) applied Mindlin's solution for horizontal force in an elastic continuum to calculate displacements at the nodes of discretized piles by the integral equation method of analysis. Similar boundary element algorithm was also adopted by Banerjee and Davies (1978). Sun (1994) and Basu et al. (2009) used variational principles to obtain analytical solutions for lateral pile displacements in elastic media. Guo and Lee (2001) assumed a stress field using the Fourier series and obtained a load transfer method for laterally loaded piles. Apart from these analytical and semi-analytical approaches, numerical analyses using the finite element method have also been carried out to analyze laterally loaded piles (Desai and Appel 1976, Bhowmik and Long 1991, Bransby 1999, Hsiung and Chen 1997). The computationally efficient Fourier series-coupled finite element method has been employed as well (Randolph 1981, Carter and Kulhawy 1992). These apart, the finite difference method (Klar and Frydman 2002, Ng and Zhang 2001), the boundary element method (Budhu and Davies 1988) and the upper-bound method of plasticity (Murff and Hamilton 1993) have been used to address the problem.

In this report, the finite element method coupled with Fourier techniques is used to analyze laterally loaded piles embedded in elastic continua. Piles with different lengths, flexibilities and boundary conditions are considered. Subsurface profiles with constant and linearly varying modulus are assumed. Additionally, a two-layer profile is considered. A parametric study is performed in which the important variables governing the pile behavior are identified. Based on the study, design equations are proposed using which pile deflection, slope and bending moment can be calculated if the correct elastic soil modulus is available. Design examples are provided to illustrate the use of the analysis.

ANALYSIS

Cylindrical piles with a lateral load F_a and moment M_a acting at the head are considered in this paper (Figure 1). The pile is described by its radius r_p , length L_p and Young's modulus E_p . The soil is described by its shear modulus G_s and Poisson's ratio ν_s . Three types of soil profiles are considered in this paper: (1) homogeneous soil in which G_s remains spatially constant, (2) heterogeneous soil in which G_s increases linearly with depth from zero value at the ground surface and (3) two-layer soil with different values of G_s that remain spatially constant within each layer (Figure 2).

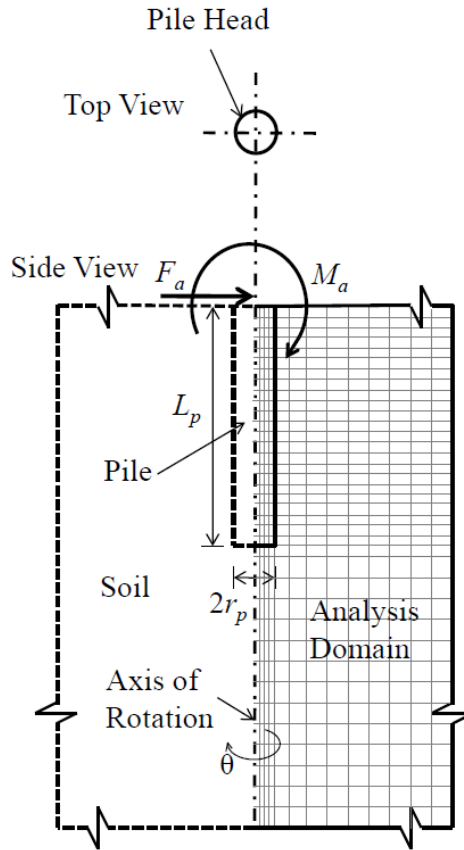


Figure 1. Schematic of analysis domain showing pile, applied load and finite element mesh

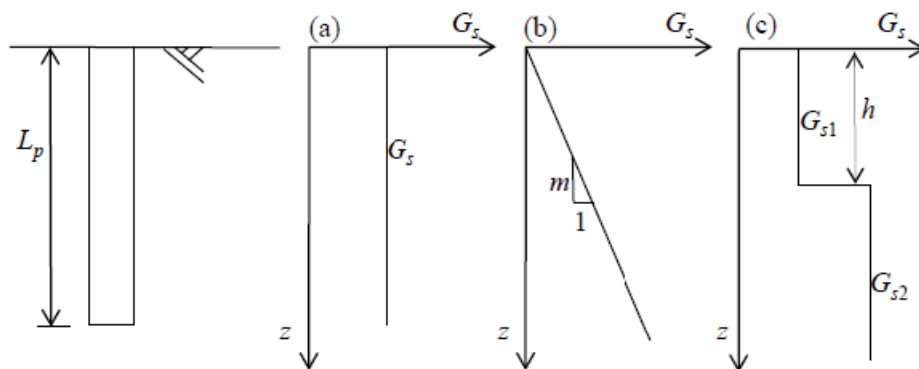


Figure 2. Plots of soil shear modulus versus depth: (a) constant stiffness with depth, (b) stiffness linearly increasing with depth with zero value at the ground surface, and (c) two-layer soil with constant stiffness in each layer

The Fourier finite element code developed by Smith and Griffiths (2004), which calculates the response of axisymmetric solids subject to non-axisymmetric loads, was used for the purpose of analysis. The domain of analysis is represented by a two-dimensional (2D) rectangular plane, which is an axisymmetric plane of the cylindrical problem geometry. The analysis domain was chosen sufficiently large so as to remove any boundary effects. The distance between the horizontal bottom boundary of the domain and the pile base was at least one pile length. The outer vertical boundary of the domain was maintained at a radial distance of at least 1.5 times the pile length from the pile-soil interface.

The analysis domain was discretized using rectangular, quadratic elements. Each element in the 2D plane represents an annulus centered on the axis of symmetry. The mesh density was different for different pile geometries. For the long piles, it was necessary to maintain a high mesh density near the pile head where the deformations are predominant. On the other hand, for short piles, a uniformly dense mesh was required throughout the entire pile length. The cases in which the stiffness varied with depth required more rows of elements so as to smoothly approximate the linear variation. About 10,000 elements were used in each mesh.

In the analysis, the applied loads are defined using harmonic functions of the angle θ representing the angular distance out from the 2D plane in the tangential direction. For example, a node on the 2D plane loaded using the zeroth harmonic represents a uniform load acting on the ring that the node represents. A node loaded using the first harmonic has a magnitude that varies sinusoidally with θ . The horizontal load and moment are created by applying horizontal and vertical loads, respectively, at

the nodes representing the pile head using the first harmonic. Using the proper harmonic, the applied horizontal load was distributed along θ in such a way that its direction always coincided with the direction of the applied horizontal load. The vertical load was distributed along θ in such a way that it was upward on one half of the pile-head section and downward on the other half, thereby creating a moment at the head.

RESULTS

Accuracy of Analysis

In order to ensure the accuracy of the Fourier finite element analysis used in this paper, selected results were compared with the results of equivalent three-dimensional (3D) finite element (FE) analysis obtained using Abaqus. The match of the pile deflection profiles between our analysis and the 3D FE analysis was perfect (with the curves falling on top of each other), which proved that the Fourier FE used in the study produces accurate results. Convergence tests were performed on all the meshes before final results were accepted.

Modification of Soil Shear Modulus

Randolph (1981) found that the effect of soil Poisson's ratio ν_s on the response of laterally loaded piles was minimal and can be adequately captured by using an equivalent shear modulus G_s^* of the elastic soil given by

$$G_s^* = G_s (1 + 0.75\nu_s) \quad (1)$$

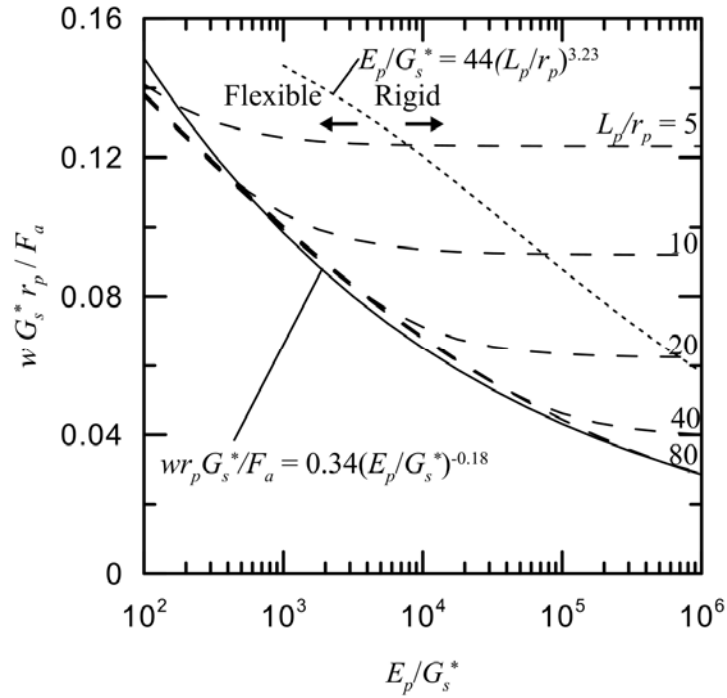
where G_s is the actual shear modulus of soil. The observation of Randolph (1981) was confirmed to be true by our analysis, and hence, G_s^* is used in our analysis to represent

the elastic properties of soil. Consequently, for soils with stiffness linearly increasing with depth z , the gradient $m = dG_s/dz$ requires modification as

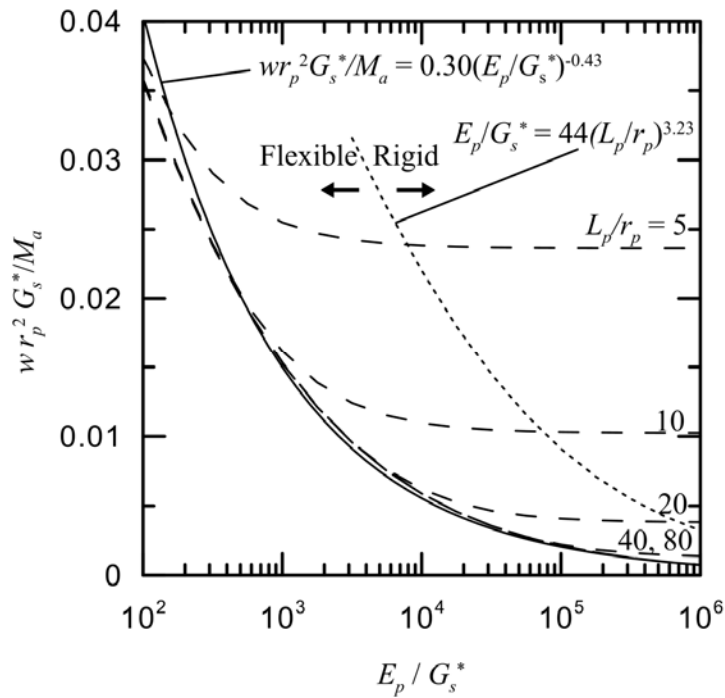
$$m^* = m(1 + 0.75\nu_s) = \frac{dG_s}{dz}(1 + 0.75\nu_s) \quad (2)$$

Effect of Relative Stiffness of Pile and Soil

The stiffness ratio E_p/G_s^* has a strong influence on the lateral pile response. For a pile of given geometry and modulus, the stiffness ratio governs whether it behaves as a flexible or a rigid pile. Figures 3(a) and (b) show the normalized head deflection w of piles with free heads as a function of the relative stiffness E_p/G_s^* due to applied force F_a and moment M_a , respectively, for different values of pile slenderness ratio L_p/r_p . The plots are generated for piles embedded in homogeneous soil profiles. For the range of E_p/G_s^* considered in this study, piles with a large slenderness ratio of 80 or greater behaves as long flexible piles with the normalized head deflection decreasing continuously with increasing E_p/G_s^* . For piles with slenderness ratio less than 80, there is a divergence from the flexible behavior towards rigid behavior as E_p/G_s^* increases. The rigid behavior is characterized by no change in the normalized pile head deflection with increasing E_p/G_s^* — at large values of E_p/G_s^* , the pile does not bend like a flexible beam but undergoes rigid translation and rotation thereby making the effect of E_p on pile behavior negligible. Consequently, the behavior of rigid piles depends only on the pile slenderness ratio (i.e., on the pile geometry). For a particular value of slenderness ratio, if the ratio E_p/G_s^* is greater than a threshold value, then the pile behaves as a rigid pile. This threshold value of E_p/G_s^* can be related to pile slenderness ratio as



(a)



(b)

Figure 3. Dimensionless pile head displacement versus stiffness ratio for free-head piles in homogeneous soil subjected to applied (a) lateral force and (b) moment at the head

$$\left(\frac{E_p}{G_s^*}\right)_{\text{RT}} = 44 \left(\frac{L_p}{r_p}\right)^{3.23} \quad (3)$$

where the subscript RT represents the rigid threshold. The plots in Figures 3(a) and (b) to the right of the threshold line (equation (3)) represent the behavior of rigid piles for which E_p/G_s^* is greater than $(E_p/G_s^*)_{\text{RT}}$.

The behavior of flexible piles, on the other hand, depends on both the relative stiffness and the slenderness ratio. However, for long piles, the length is so large that the pile-base conditions do not affect the behavior of the pile head. For such long and slender piles, the lateral behavior can be adequately expressed in terms of E_p/G_s^* alone. As shown in Figures 3(a) and (b), the pile with $L_p/r_p \geq 80$ behaves like a long pile. The head deflection for such long piles can be expressed algebraically by fitting a curve through the long pile response plots shown in Figures 3(a) and (b) as

$$w = 0.34 \frac{F_a}{G_s^* r_p} \left(\frac{E_p}{G_s^*}\right)^{-0.18} + 0.30 \frac{M_a}{G_s^* r_p^2} \left(\frac{E_p}{G_s^*}\right)^{-0.43} \quad (4)$$

Similarly, the head rotation (slope) of long flexible piles is independent of pile slenderness ratio and can be expressed as

$$\left(\frac{dw}{dz}\right)_{z=0} = 0.28 \frac{F_a}{G_s^* r_p^2} \left(\frac{E_p}{G_s^*}\right)^{-0.43} + 0.90 \frac{M_a}{G_s^* r_p^3} \left(\frac{E_p}{G_s^*}\right)^{-0.72} \quad (5)$$

The response of piles embedded in soil profiles in which the shear modulus increases linearly with depth from a zero value at the surface is similar to those observed for piles in homogeneous profiles described above. For such linearly varying profiles, the relative stiffness of pile and soil is adequately represented by the ratio $E_p/m^* r_p$ (Randolph 1981). Figures 4(a) and (b) show the corresponding normalized head

deflection of free-head piles subjected to a lateral force F_a and moment M_a at the head.

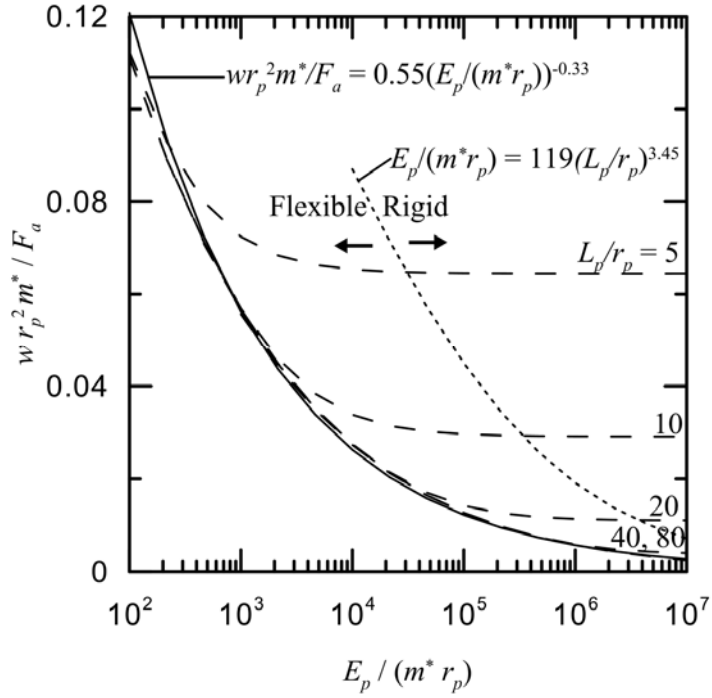
The threshold $(E_p/m^* r_p)_{RT}$, exceeding which the piles behave as rigid piles, is given by

$$\left(\frac{E_p}{m^* r_p}\right)_{RT} = 119 \left(\frac{L_p}{r_p}\right)^{3.45} \quad (6)$$

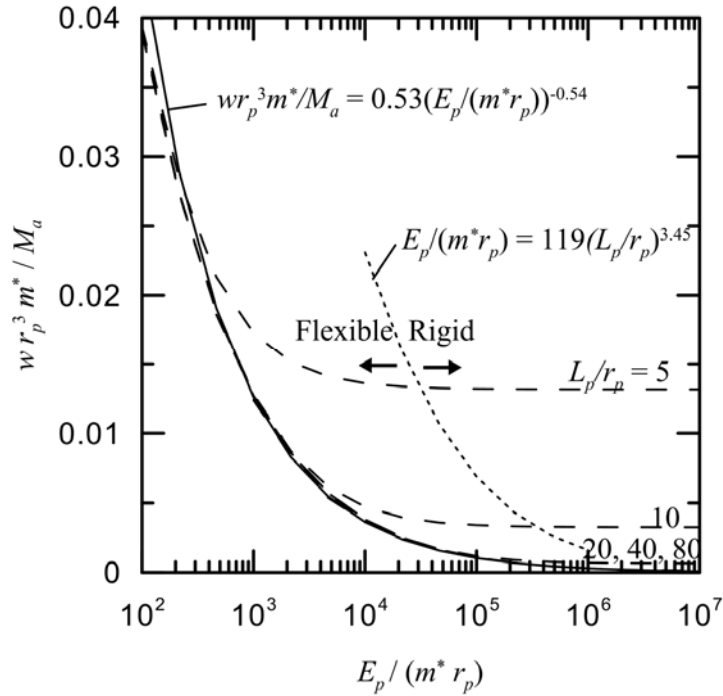
The head deflection and slope of the long flexible piles, for which $(E_p/m^* r_p) < (E_p/m^* r_p)_{RT}$, are given by the fitted equations

$$w = 0.55 \frac{F_a}{m^* r_p^2} \left(\frac{E_p}{m^* r_p}\right)^{-0.33} + 0.53 \frac{M_a}{m^* r_p^3} \left(\frac{E_p}{m^* r_p}\right)^{-0.54} \quad (7)$$

$$\left(\frac{dw}{dz}\right)_{z=0} = 0.50 \frac{F_a}{m^* r_p^3} \left(\frac{E_p}{m^* r_p}\right)^{-0.54} + 1.23 \frac{M_a}{m^* r_p^4} \left(\frac{E_p}{m^* r_p}\right)^{-0.78} \quad (8)$$



(a)



(b)

Figure 4. Dimensionless pile head displacement versus relative stiffness due to applied (a) lateral force and (b) moment at the head of free-head piles in soil profiles in which modulus increases linearly with depth

Pile heads are rarely free to translate and rotate as piles are most of the time attached to a structural element above. If a cap is present, the head rotation is significantly restrained and it is customary to assume that there is zero rotation at the head. The response of such fixed-head piles are shown in Figure 5 for homogeneous soil profiles and in Figure 6 for heterogeneous soil profiles in which the modulus increases linearly with depth from zero at the surface. The general trend of the normalized head deflection versus stiffness ratio plots in Figures 5 and 6 is similar to that observed for the corresponding cases of free-head piles described above.

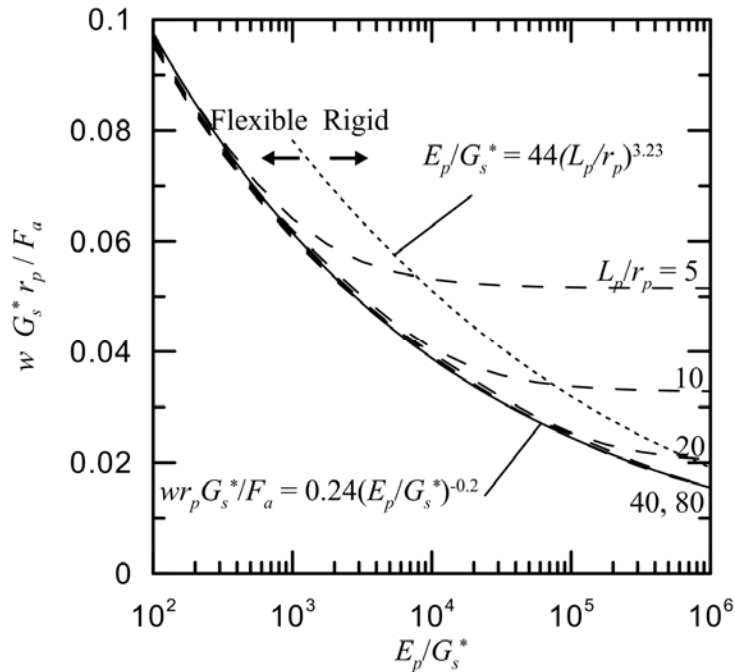


Figure 5. Dimensionless pile head displacement versus stiffness ratio for fixed-head piles in homogeneous soil profiles subjected to applied lateral force at the head

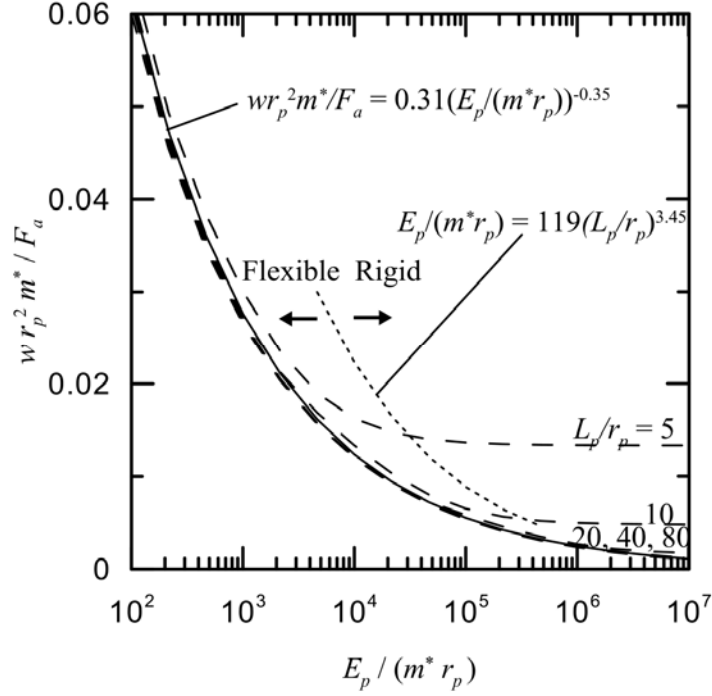


Figure 6. Dimensionless pile head displacement versus relative stiffness due to applied lateral force at the head of fixed-head piles in soil profiles in which the modulus increases linearly with depth

The fixed-head piles with $(E_p/G_s^*) > (E_p/G_s^*)_{RT}$ undergo rigid translation due to application of the applied force F_a , and do not exhibit any rigid rotation. Equations (3) and (6) describing $(E_p/G_s^*)_{RT}$ for free-head piles in homogeneous and linearly varying soil profiles, respectively, were found to be valid for the corresponding cases of fixed-head piles as well. The head deflection of long, flexible, fixed-head piles in homogeneous soil is obtained by fitting a curve to the plots corresponding to long piles in Figure 5 as

$$w = 0.24 \frac{F_a}{G_s^* r_p} \left(\frac{E_p}{G_s^*} \right)^{-0.2} \quad (9)$$

The fitted equation for the head deflection of fixed-head long piles in soil with linearly varying modulus is obtained from Figure 6 as

$$w = 0.31 \frac{F_a}{m^* r_p} \left(\frac{E_p}{m^* r_p} \right)^{-0.35} \quad (10)$$

Note that the head deflection for fixed-head piles can be obtained from the equations of head deflection and slope for free-head piles (i.e., from equations (4) and (5) for homogeneous soils and from equations (7) and (8) for linearly varying soils) by equating the slope to zero to obtain an expression of M_a in terms of F_a and then substituting the resulting expression in the equation of deflection to obtain the final value. However, we observed that the resulting values of fixed-head deflection did not accurately match the simulated results because the algebraic manipulations of the curve-fitted equations increased the errors in the calculations. The fitted equations (9) and (10) were found to better predict the simulated results.

In addition to pile deflection, the bending moments at pile cross sections are important for the design of piles. When a moment is applied at a free pile head, the maximum bending moment M_{max} is equal to the applied moment and occurs at the pile head (Randolph 1981). The maximum bending moment due to an applied horizontal force on free-head piles occurs at a finite depth below the ground surface. Figures 7 and 8 show the normalized maximum bending moment in free-head piles, due to an applied horizontal force at the head, as a function of the relative stiffness in homogeneous and linearly varying soil profiles, respectively. For long flexible piles, M_{max} is independent of the pile slenderness ratio and can be expressed as (Randolph 1981)

$$M_{max} = 0.2 F_a r_p \left(\frac{E_p}{G_s^*} \right)^{0.29} \quad (11)$$

for homogeneous soil profiles and as

$$M_{max} = 0.4F_a r_p \left(\frac{E_p}{m^* r_p} \right)^{0.22} \quad (12)$$

for soil profiles in which the modulus increases linearly with depth from zero at the surface. For shorter piles, M_{max} depends on pile slenderness ratio and, as the relative stiffness increases, M_{max} deviates from the trend followed by long piles. At large values of the stiffness ratio, M_{max} of shorter piles becomes independent of the stiffness ratio indicating a rigid behavior.

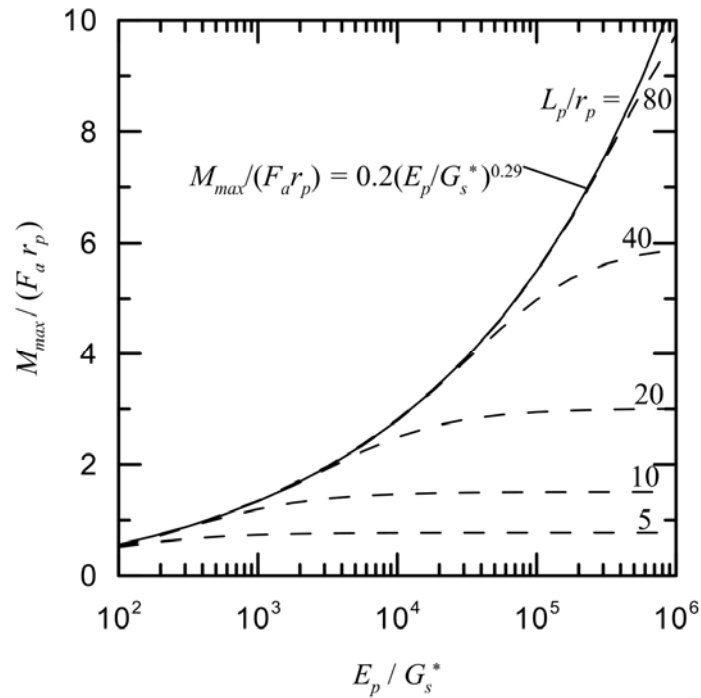


Figure 7. Dimensionless maximum bending moment versus stiffness ratio for free-head piles in homogeneous soil and subjected to an applied horizontal force at the head

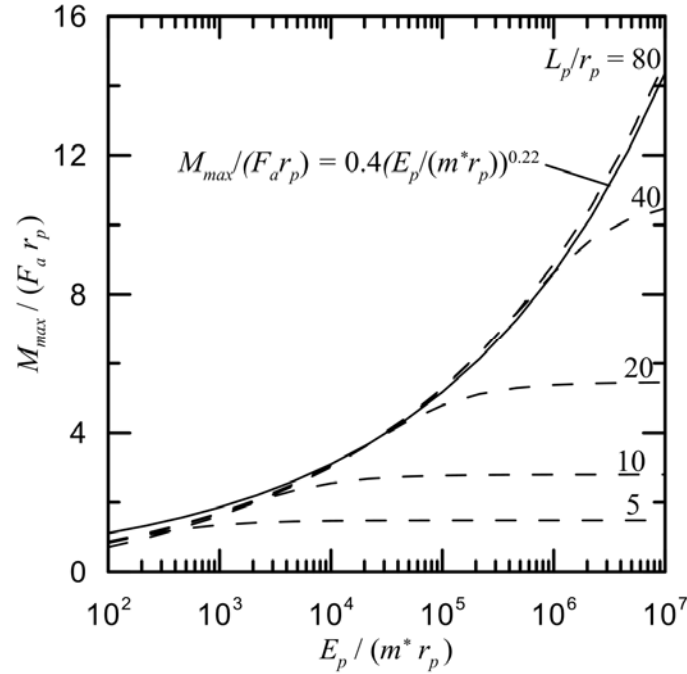


Figure 8. Dimensionless maximum bending moment versus relative stiffness for free-head piles in linearly varying soil and subjected to an applied horizontal force at the head

Effect of Pile Slenderness Ratio

It is clear from the above discussion that the behavior of rigid piles and of flexible piles with moderately long lengths depends on pile slenderness ratio L_p/r_p . Thus, the effect of slenderness ratio on pile behavior is investigated further. The normalized pile head deflection due to applied force and moment are plotted as a function of L_p/r_p in Figures 9(a) and (b), respectively, for different values of E_p/G_s^* . These plots are generated for free-head piles in homogeneous soil profiles. For the range of slenderness ratio considered in the study, a value of $E_p/G_s^* = 10^5$ or greater produced rigid piles. For piles with E_p/G_s^* less than 10^5 , the pile response deviates from the rigid behavior and there is a threshold value of L_p/r_p exceeding which the normalized head deflection becomes independent of the slenderness ratio implying that the behavior is that of

flexible long piles. This threshold value of L_p/r_p represents the critical slenderness ratio $(L_p/r_p)_C$ and can be related to the stiffness ratio E_p/G_s^* as (Randolph 1981)

$$\left(\frac{L_p}{r_p}\right)_C = 2\left(\frac{E_p}{G_s^*}\right)^{0.29} \quad (13)$$

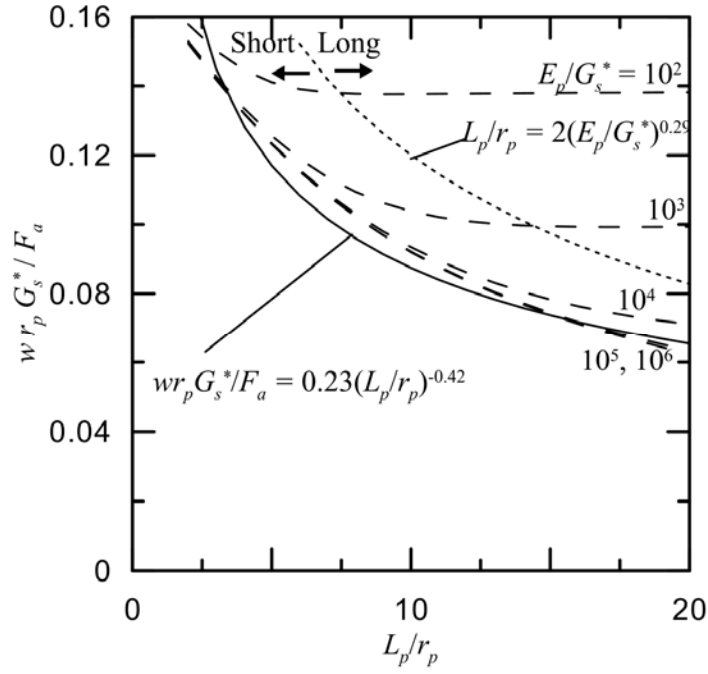
Piles with $(L_p/r_p) > (L_p/r_p)_C$ behave as long flexible piles and the length that produces the slenderness ratio equal to $(L_p/r_p)_C$ is often referred to as the critical length L_c of pile. L_c essentially represents a threshold length such that any additional pile length does not have any impact on the lateral pile response. Equation (13) indicates that whether a pile behaves as a flexible long pile or not depends not only on its physical length but also on the relative stiffness E_p/G_s^* .

Since the behavior of rigid piles depends only on pile slenderness ratio, Figures 9(a) and (b) can be used to obtain a fitted algebraic equation for pile head deflection of free-head, rigid piles in homogeneous soil as

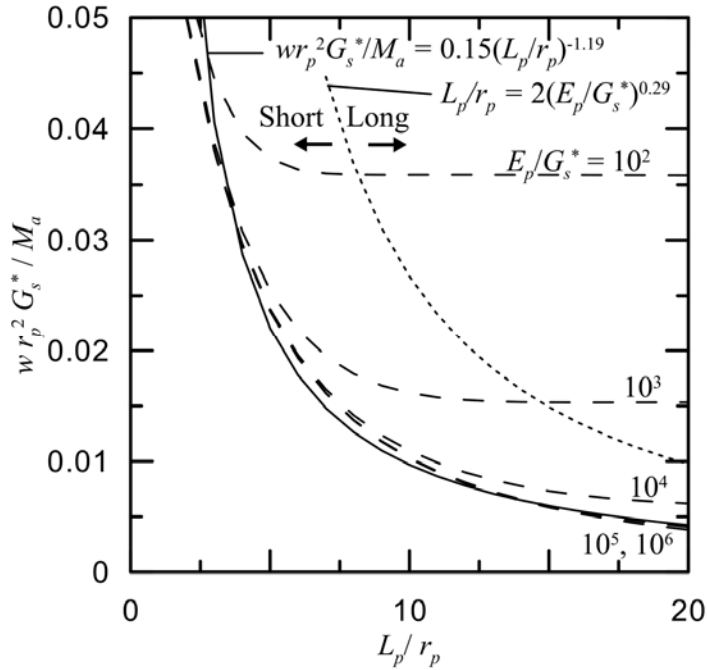
$$w = 0.23\left(\frac{F_a}{G_s^* r_p}\right)\left(\frac{L_p}{r_p}\right)^{-0.42} + 0.15\left(\frac{M_a}{G_s^* r_p^2}\right)\left(\frac{L_p}{r_p}\right)^{-1.19} \quad (14)$$

The rotation of free-head, rigid piles in homogeneous soil can be similarly expressed as

$$\left(\frac{dw}{dz}\right)_{z=0} = 0.15\left(\frac{F_a}{G_s^* r_p^2}\right)\left(\frac{L_p}{r_p}\right)^{-1.19} + 0.21\left(\frac{M_a}{G_s^* r_p^3}\right)\left(\frac{L_p}{r_p}\right)^{-2.10} \quad (15)$$



(a)



(b)

Figure 9. Dimensionless pile head displacement versus slenderness ratio for free-head piles in homogeneous soil profiles subjected to applied (a) lateral force and (b) moment at the head

The normalized head deflection versus slenderness ratio relationships for free-head piles in soil profiles with shear modulus increasing linearly with depth from zero at the surface are similar to those obtained for homogeneous profiles. Figures 10(a) and (b) show the plots for applied horizontal force and moment, respectively. Based on the figures, the critical slenderness ratio of free-head piles in linearly varying soil profile can be obtained as (Randolph 1981)

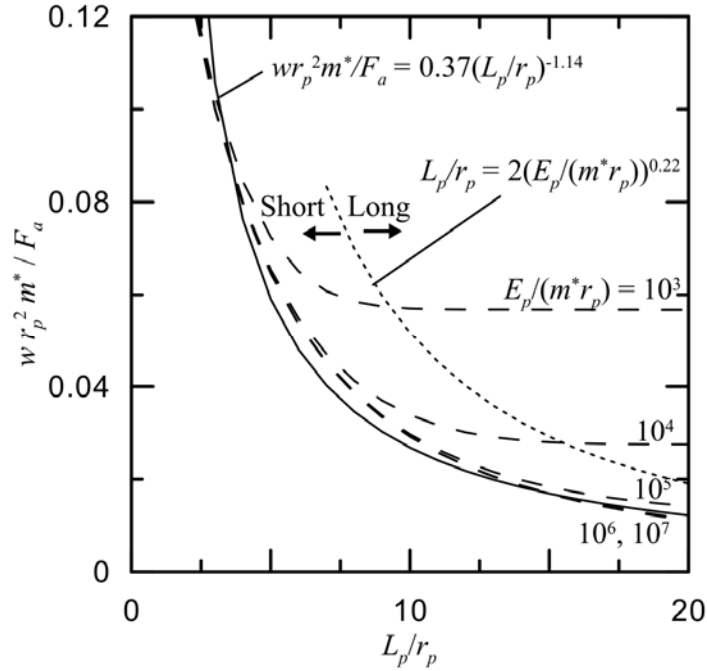
$$\left(\frac{L_p}{r_p}\right)_c = 2 \left(\frac{E_p}{m^* r_p}\right)^{0.22} \quad (16)$$

Also, the head deflection of free-head rigid piles in linearly varying soil is obtained from Figures 10(a) and (b) as

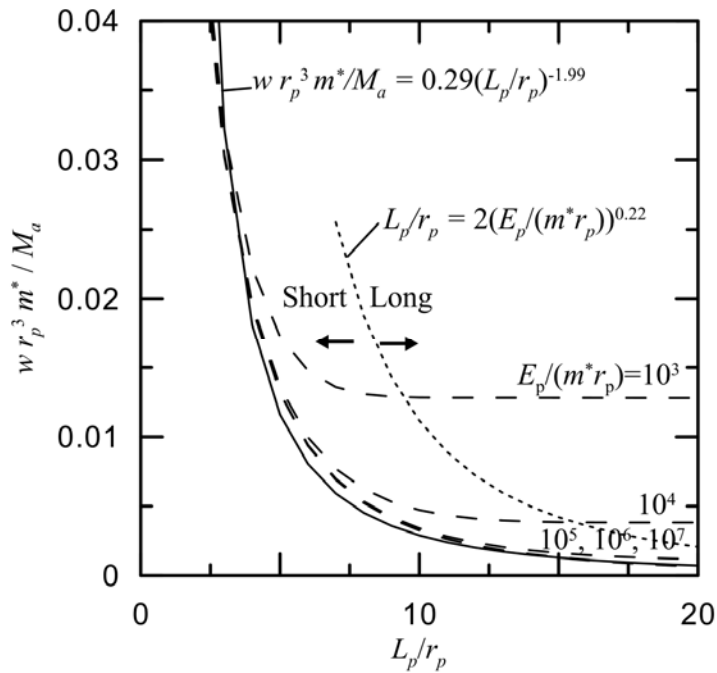
$$w = 0.37 \frac{F_a}{m^* r_p^2} \left(\frac{L_p}{r_p}\right)^{-1.14} + 0.29 \frac{M_a}{m^* r_p^3} \left(\frac{L_p}{r_p}\right)^{-1.99} \quad (17)$$

The rotation of free-head rigid piles is similarly obtained as

$$\left(\frac{dw}{dz}\right)_{z=0} = 0.29 \frac{F_a}{m^* r_p^3} \left(\frac{L_p}{r_p}\right)^{-1.99} + 0.33 \frac{M_a}{m^* r_p^4} \left(\frac{L_p}{r_p}\right)^{-2.93} \quad (18)$$



(a)



(b)

Figure 10. Dimensionless pile head displacement versus slenderness ratio due to applied (a) lateral force and (b) moment at the head of free-head piles in soil profiles with modulus increasing linearly with depth from zero at the surface

The normalized head deflection for fixed-head piles as a function of pile slenderness ratio is plotted in Figures 11 and 12 for homogeneous and linearly varying soil profiles, respectively. The trends exhibited by the fixed-head piles are similar to those by the free-head piles. Equations (13) and (16) describing $(L_p/r_p)_C$ for free-head piles in homogeneous and linearly varying soil profiles, respectively, were found to be valid for the corresponding cases of fixed-head piles as well. Also, the fitted equation for head deflection (translation) of fixed-head rigid piles in homogeneous soil is obtained from Figure 11 as

$$w = 0.14 \left(\frac{F_a}{G_s^* r_p} \right) \left(\frac{L_p}{r_p} \right)^{-0.65} \quad (19)$$

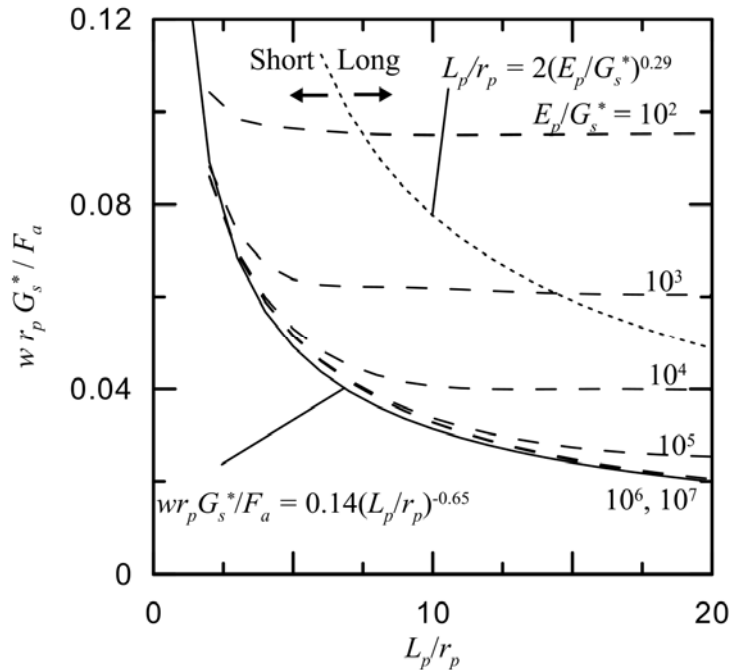


Figure 11. Dimensionless pile head displacement versus slenderness ratio for fixed-head piles in homogeneous soil profiles subjected to applied lateral force at the head

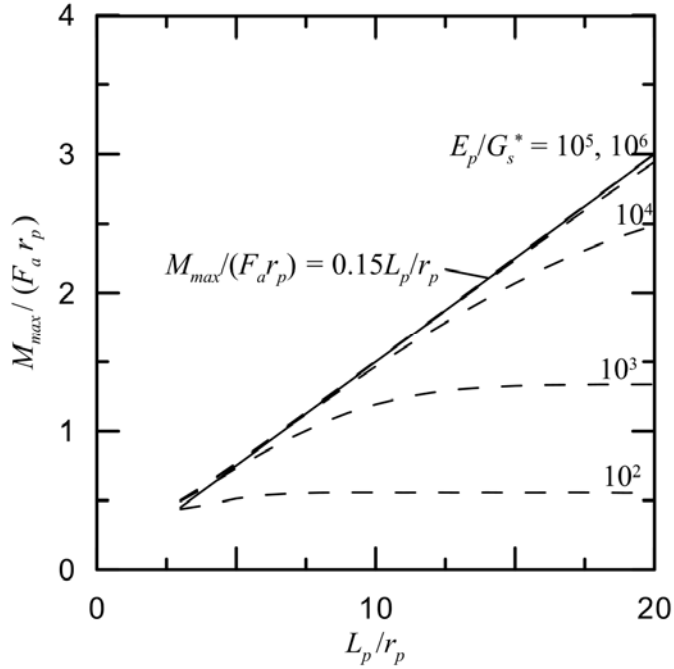


Figure 13. Dimensionless maximum bending moment versus slenderness ratio for free-head piles in homogeneous soil and subjected to an applied horizontal force at the head

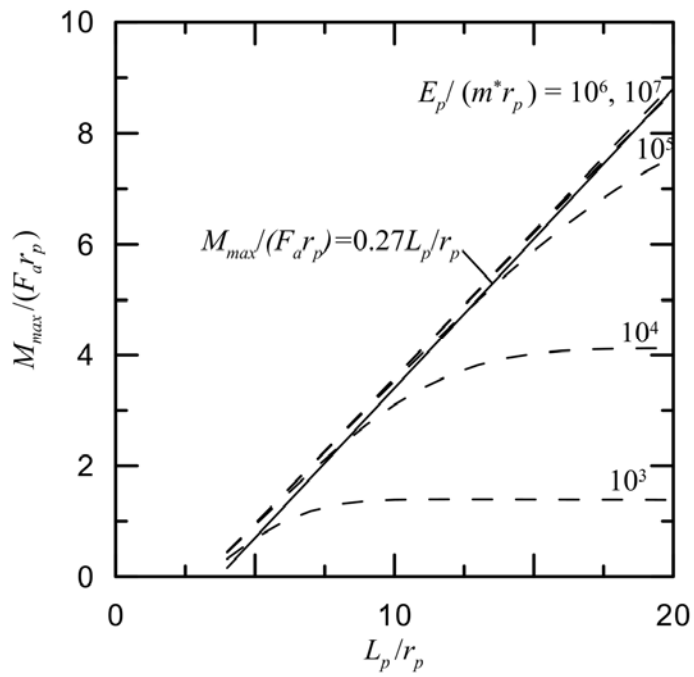


Figure 14. Dimensionless maximum bending moment versus slenderness ratio for free-head piles in linearly varying soil and subjected to an applied horizontal force at the head

$$M_{max} = 0.15 F_a r_p \left(\frac{L}{r_p} \right) = 0.15 F_a L_p \quad (21)$$

for homogeneous profiles and by

$$M_{max} = 0.27 F_a r_p \left(\frac{L}{r_p} \right) = 0.27 F_a L_p \quad (22)$$

for linearly varying profiles.

The fitted equations of pile head deflection, rotation and maximum bending moment given above are valid for either rigid piles or for flexible long piles. In order to use these equations, first a check as to whether a pile behaves as a rigid or a long flexible pile should be done by calculating the rigid threshold relative stiffness and the critical slenderness ratio. If a pile does not fall in the category of rigid or flexible long piles, then it is a flexible pile of intermediate length. For these piles with intermediate length, no simple equation can be proposed as their behavior depends on both the pile slenderness ratio and relative pile-soil stiffness, and appropriate normalizations with respect to both these parameters are difficult to obtain. Thus, for these intermediate-sized piles, the head deflection, rotation and maximum bending moment may be estimated from the plots given in Figures 3-14.

Piles in Two-Layer Profiles

Often, soil profiles have discrete layers with distinct properties. For such profiles, the results obtained above are not strictly valid. Although an exhaustive study with different possible soil layering is beyond the scope of this paper, a simple case of two-layer profile is investigated here. The two-layer profile is characterized by the equivalent shear moduli G_{s1}^* and G_{s2}^* of the top (first) and the underlying (bottom) layers,

respectively, and by the thickness h of the top layer (Figure 2(c)). The bottom layer is assumed to extend to great depth.

Figure 15 shows the normalized head deflection of long, flexible free-head piles in two-layer soil profiles due to applied lateral force at the head as a function of the relative stiffness E_p/G_{s1}^* . The deflections in these plots are normalized with respect to the shear modulus G_{s1}^* of the top layer the thickness h of which is fixed at half the critical pile length L_c . The plots are generated for different values of soil stiffness ratio G_{s2}^*/G_{s1}^* with a fixed value of G_{s1}^* . Thus, for the case with $G_{s2}^*/G_{s1}^* = 0.5$, the bottom layer is made weaker than the top layer while, for the case with $G_{s2}^*/G_{s1}^* = 2.0$, the bottom layer is made twice as strong as the top layer. For a fixed value of stiffness of the top layer, a weaker bottom layer results in greater head deflection while a stronger bottom layer results in less head deflection than that of the corresponding homogeneous case. This difference in head deflection, however, decreases with increasing E_p/G_{s1}^* .

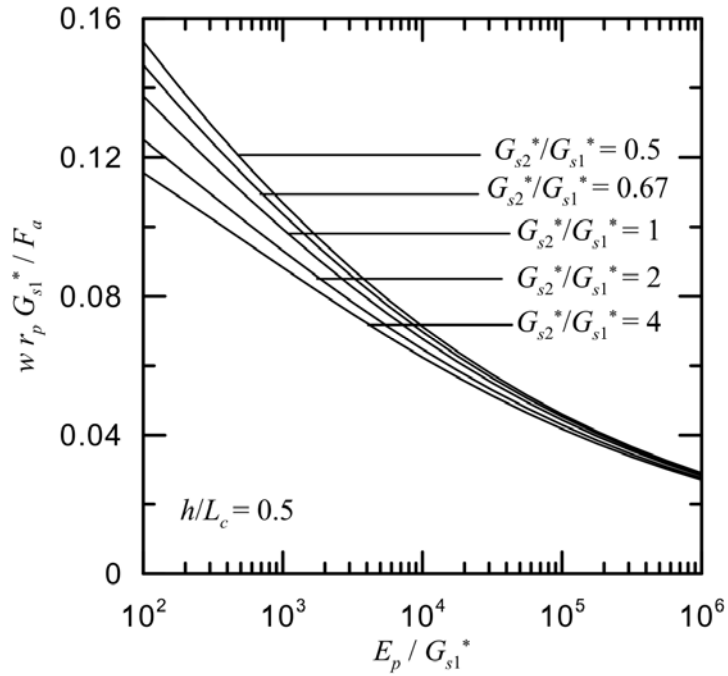


Figure 15. Dimensionless pile head displacement versus relative stiffness for long, flexible and free-head piles in two-layer soil due to applied lateral force

Figure 16 shows the effect of the thickness h of the top layer on the response of free-head long piles in two-layer soil. If the bottom layer is weak as in the case with $G_{s2}^* / G_{s1}^* = 0.5$, then a greater h/L_c produces less head deflection while the reverse is true for $G_{s2}^* / G_{s1}^* = 2.0$.

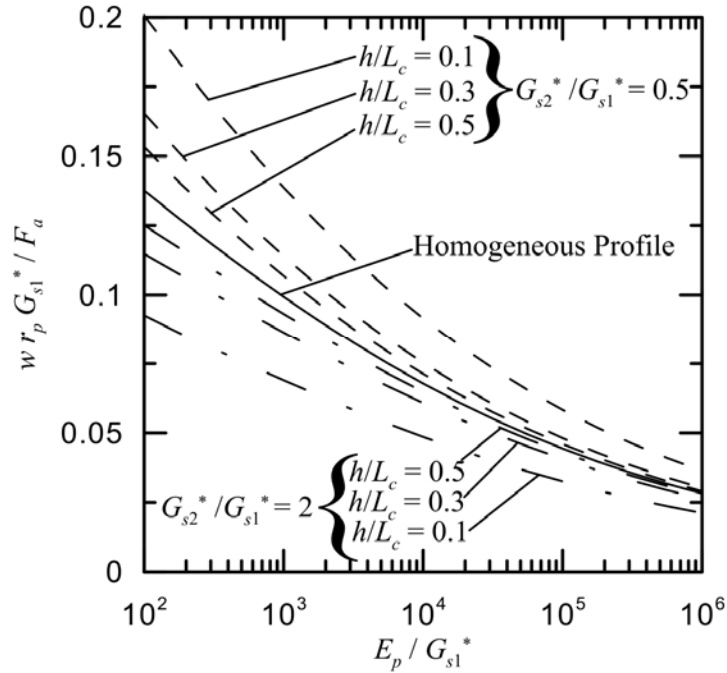


Figure 16. Dimensionless pile head displacement versus relative stiffness for long, flexible and free-head piles in two-layer soil due to applied lateral force showing the effect of layer thickness

Figures 17 and 18 show the response of rigid piles in two-layer soil. In these figures, the pile head deflection, normalized with respect to G_{s1}^* , is plotted as a function of pile slenderness ratio L_p/r_p . Figure 17 shows that, for a fixed top layer with thickness $h = 0.5L_p$ and stiffness G_{s1}^* , the head deflection decreases with increasing G_{s2}^*/G_{s1}^* . Figure 18 shows that, if the thickness of the top layer increases, then head deflection increases if the bottom layer is stronger than the top layer, while the head deflection decreases as the thickness of the top layer increases if the bottom layer is weaker than the top layer.

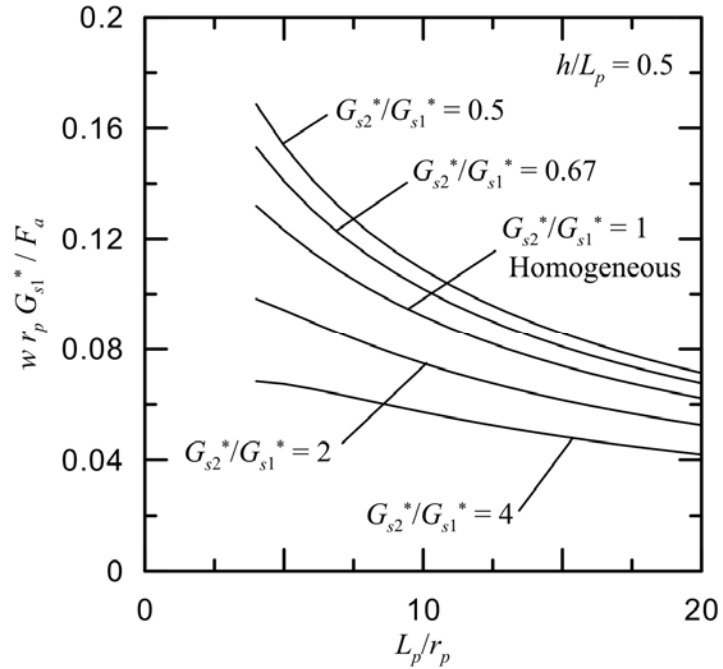


Figure 17. Dimensionless pile head displacement versus slenderness ratio for rigid, free-head piles in two-layer soil due to applied lateral force showing the effect of soil stiffness ratio

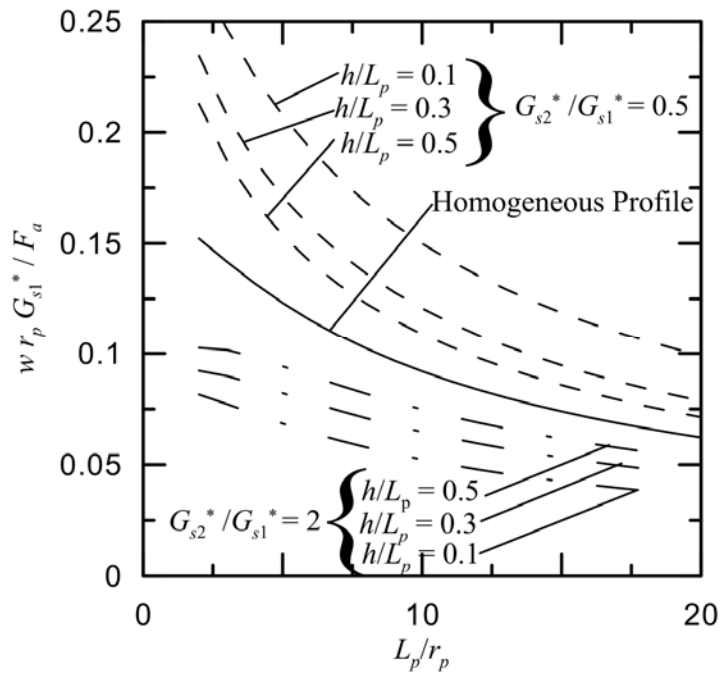


Figure 18. Dimensionless displacement versus slenderness ratio for rigid, free-head piles in two-layer soil due to applied lateral force showing the effect of layer thickness

Design Examples

Two design examples are considered in this section — one with constant modulus and the other with linearly varying modulus. In both the examples it is assumed that the piles are first designed against axial loads and then checked against tolerable lateral deflections.

A single drilled shaft is to be designed in a homogeneous clay layer with undrained shear strength $s_u = 150$ kPa. From the design considerations against axial loads it was found that a pile length of 15 m and a diameter of 600 mm is adequate. A lateral load of 300 kN and moment of 100 kN-m act on the pile. It is necessary to restrict the head deflection to within 25 mm. Assuming undrained conditions it is reasonable to choose clay Poisson's ratio $\nu_s = 0.45$. The Young's modulus E_s of clay can be estimated from the relationship $E_s = 500s_u$ (Selvadurai 1979) as 75,000 kPa. Thus, for the soil profile in question, $G_s = 0.5 E_s / (1 + \nu_s) = 25862$ kPa and $G_s^* = G_s (1 + 0.75\nu_s) = 34590$ kPa. Since drilled shafts are made of lightly reinforced concrete, $E_p = 24 \times 10^6$ kPa is a reasonable assumption, which makes $E_p/G_s^* = 694$. The pile slenderness ratio $L_p/r_p = 50$. Since the rigid threshold $(E_p/G_s^*)_{RT} = 44 \times 50^{3.23} = 13524642$ is much greater than the E_p/G_s^* of the pile, it behaves as a flexible member. The critical slenderness ratio $(L_p/r_p)_C = 2 \times 69^{0.29} = 6.8$ is less than the actual pile slenderness ratio. Therefore, the drilled shaft behaves as a long pile. Consequently, equation (4) can be used to estimate the pile head deflection — the estimated head deflection is 3.6 mm. Thus, the estimated lateral head deflection is less than the tolerable deflection of 25 mm, which makes the design satisfactory.

As a second example, a driven concrete pile, attached to a cap, is to be designed in a sandy soil deposit. Considering axial capacity, the pile has the following dimensions $L_p = 20$ m and $r_p = 0.2$ m. A lateral force of 500 kN acts at the pile head. The tolerable lateral head deflection is 25 mm. The soil profile consists of very loose deposit near the ground surface although the relative density increases gradually with depth. The increase in the relative density with depth can be assumed to be approximately linear and a relative density of 80% was observed at a depth of 30 m. For dense sands, the Young's modulus E_s can be conservatively assumed to be 75,000 kPa (Selvadurai 1979). Since the sand near the ground surface is very loose, the Young's modulus can be assumed to be zero at the surface. The Poisson's ratio ν_s of sand can be reasonably assumed to be 0.2 (Selvadurai 1979). This makes the shear modulus $G_s = 31250$ kPa at a depth of 30 m and zero at the ground surface. Thus, the gradient $m = dG_s/dz$ of the linear variation of shear modulus is equal to 1042 kPa/m and $m^* = m(1 + 0.75\nu_s) = 1198$ kPa/m. Since driven concrete piles are heavily reinforced, $E_p = 25 \times 10^6$ kPa is a reasonable assumption. Thus, for this pile, $L_p/r_p = 100$, $E_p/m^* r_p = 104340$, $(E_p/m^* r_p)_{RT} = 945250599$ and $(L_p/r_p)_C = 25.4$. Therefore, the pile falls under the category of long, flexible and fixed-head piles. The lateral head deflection is calculated as 11.3 mm using equation (10). Since the estimated head deflection is less than the tolerable deflection of 25 mm, the design is acceptable.

CONCLUSIONS

Laterally loaded piles embedded in elastic soil are analyzed using the Fourier finite element analysis. Homogeneous soil profiles in which the soil modulus remains spatially constant, heterogeneous profiles in which the modulus increases linearly with

depth from zero value at the ground surface, and two-layer soil profiles with different soil moduli within each layer are considered in the analysis. The effects of relative stiffness of pile and soil and of pile slenderness ratio on pile head deflection, rotation and maximum bending moment were investigated.

Three distinct behavior regimes were identified from the results. The piles with relative pile-soil stiffness greater than a threshold value behaved as rigid members. For these piles, the response depends only on the pile slenderness ratio L_p/r_p — the normalized head deflection decreases with increasing slenderness ratio. The piles with relative stiffness less than the threshold value behaved as flexible piles. When the slenderness ratio of flexible piles is greater than the critical slenderness ratio, the piles behave as long piles. For the long flexible piles, the behavior depends only on the relative pile-soil stiffness — the head deflection decreases as the relative stiffness increases. The behavior of flexible piles with moderate lengths, for which the slenderness ratio is less than the critical slenderness ratio, is dependent on both the relative stiffness and slenderness ratio. For these moderate-length piles, the head deflection decreases with increasing relative stiffness and with increasing slenderness ratio.

Piles subjected to applied moment at the head (which includes free- and fixed-head piles) have the maximum bending moment acting at the head — the maximum bending moment is equal to the applied moment. The maximum bending moment due to an applied horizontal force on free-head piles occurs at a finite depth below the ground surface. The normalized maximum bending moment of free-head flexible piles increases

with increase in the relative pile-soil stiffness. For rigid free-head piles, the normalized bending moment increases with increase in the pile slenderness ratio.

For piles in two-layer soil, there is an effect on the pile response of the thickness of the top layer and of the stiffness ratio G_{s2}^*/G_{s1}^* of the two layers. Lateral pile displacement increases not only if the stiffness of the top layer decreases but also if the stiffness of the bottom layer decreases. For a weaker top layer, the pile displacement increases as the thickness of the top layer increases. However, the effect of the bottom layer is marginal if the thickness of the top layer is very large.

Based on the above study, algebraic equations describing the pile head deflection, rotation and bending moment were developed by fitting the results of the finite element analyses. The equations were developed for rigid piles and for long flexible piles and can be readily used in design. Such equations could not be proposed for flexible piles of moderate lengths; for these piles, the plotted figures may be used as design charts. The use of the analysis in design is illustrated with the help of two numerical examples.

REFERENCES

- Banerjee, P. K. and Davies, T. G. (1978). The behaviour of axially and laterally loaded single piles embedded in nonhomogeneous soils. *Géotechnique* **28**, No. 3, 309–326.
- Basu, D., Salgado, R. and Prezzi, M. (2009). A continuum-based model for analysis of laterally loaded piles in layered soils. *Géotechnique*, **59**, No 2, 127 - 140
- Bhowmik, S., and Long J. H. (1991). An analytical investigation of the behavior of laterally loaded piles. *Proc. Geotech. Eng. Congress, ASCE* **2**, No. 27, 1307-1318.
- Bransby, M. F. (1999). Selection of p - y curves for the design of single laterally loaded piles. *Int. J. Numer. Anal. Methods Geomech.* **23**, No. 15, 1909–1926.

- Budhu, M. and Davies, T. G. (1988). Analysis of laterally loaded piles in soft clays. *J. Geotech. Engng Div. ASCE* **114**, No. 1, 21–39.
- Carter, J.P. and Kulhawy, F.H. (1992) Analysis of laterally loaded shafts in rock. *Journal of Geotechnical Engineering* **118**, No. 6, 839-855
- Desai, C. S. & Appel, G. C. (1976). 3-D analysis of laterally loaded structures. *Proceedings of the 2nd international conference on Num. Meth. Geomech. Blacksburg, VA.* **1**, 405-418.
- Guo, W. D. and Lee, F. H. (2001). Load transfer approach for laterally loaded piles. *Int. J. Numer. Anal. Methods Geomech.* **25**, No. 11, 1101–1129.
- Hsiung, Y., and Chen, Y. (1997). Simplified method for analyzing laterally loaded single piles in clays. *Journal of Geotechnical and Geoenvironmental Engineering* **123**, No. 11, 1018-1028.
- Kim, T. K., Kim, N-K, Lee, W. J. & Kim, Y. S. (2004). Experimental load-transfer curves of laterally loaded piles in Nak-Dong river sand. *J. Geotech. Geoenv. Engng., Am. Soc. Civ. Engrs.* **130**, No. 4, 416-425.
- Klar, A. and Frydman, S. (2002). Three-dimensional analysis of lateral pile response using two-dimensional explicit numerical scheme. *J. Geotech. Geoenviron. Engng ASCE* **128**, No. 9, 775– 784.
- Matlock, H., and Reese, L. C. (1960). Generalized solutions for laterally loaded piles. *J. Soil Mech. Found. Div., ASCE* **86**, No. 5, 63-91.
- Matlock, H. (1970). Correlations for design of laterally loaded piles in soft clay. *Proc. 2nd Offshore Technol. Conf., Houston, TX* **1**, 577–594.

- McClelland, B. and Focht, J. A. Jr (1958). Soil modulus for laterally loaded piles. *Trans. ASCE* **123**, 1049–1063.
- Murff, J.D., and Hamilton, J.M. (1993). P-Ultimate for undrained analysis of laterally loaded piles. *ASCE Journal of Geotechnical Engineering* **119**, No. 1, 91-107.
- Ng, C. W. W. and Zhang, L. M. (2001). Three-dimensional analysis of performance of laterally loaded sleeved piles in sloping ground. *J. Geotech. Geoenviron. Engng ASCE* **127**, No. 6, 499–509.
- Poulos, H. G. (1971a). Behavior of laterally loaded piles: I – single piles. *J. Soil Mech. Found. Div. ASCE* **97**, No. SM5, 711–731.
- Poulos, H. G. (1971b). Behavior of laterally loaded piles: III – socketed piles. *J. Soil Mech. Found. Div. ASCE* **98**, No. SM4, 341–360.
- Randolph, M. F. (1981). The response of flexible piles to lateral loading. *Géotechnique* **31**, No. 2, 247-259.
- Reese, L. and Cox, W. (1968). Soil behavior from analysis of tests of uninstrumented piles under lateral loading. *Proc. Seventy-first Annual Meeting, ASTM, San Francisco, CA*, 161-176.
- Reese, L. C., Cox, W. R. and Koop, F. D. (1974). Analysis of laterally loaded piles in sand. *Proc. 6th Offshore Technol. Conf., Houston, TX* **2**, 473–483.
- Reese, L. C., Cox, W. R. and Koop, F. D. (1975). Field testing and analysis of laterally loaded piles in stiff clay. *Proc. 7th Offshore Technol. Conf., Houston, TX* **2**, 671–690.
- Selvadurai, A. P. S. (1979). *Elastic Analysis of Soil-Foundation Interaction*, Elsevier.
- Smith, I.M. and Griffiths, D.V. (2004) *Programming the Finite Element Method*, 4th ed. Wiley, West Sussex.

Sun, K. (1994). Laterally loaded piles in elastic media. *J. Geotech. Engng ASCE* **120**, No. 8, 1324–1344.